Integration of the *Aedes aegypti* Mosquito Genetic Linkage and Physical Maps

S. E. Brown,* D. W. Severson,†,[1] L. A. Smith† and D. L. Knudson*

**Department of Bioagricultural Sciences and Pest Management, College of Agricultural Sciences, Colorado State University, Fort Collins, Colorado 80523 and †Department of Animal Health and Biomedical Sciences, University of Wisconsin, Madison, Wisconsin 53706*

Manuscript received August 30, 2000
Accepted for publication December 1, 2000

ABSTRACT

Two approaches were used to correlate the *Aedes aegypti* genetic linkage map to the physical map. STS markers were developed for previously mapped RFLP-based genetic markers so that large genomic clones from cosmid libraries could be found and placed to the metaphase chromosome physical maps using standard FISH methods. Eight cosmids were identified that contained eight RFLP marker sequences, and these cosmids were located on the metaphase chromosomes. Twenty-one cDNAs were mapped directly to metaphase chromosomes using a FISH amplification procedure. The chromosome numbering schemes of the genetic linkage and physical maps corresponded directly and the orientations of the genetic linkage maps for chromosomes 2 and 3 were inverted relative to the physical maps. While the chromosome 2 linkage map represented essentially 100% of chromosome 2, ~65% of the chromosome 1 linkage map mapped to only 36% of the short *p*-arm and 83% of the chromosome 3 physical map contained the complete genetic linkage map. Since the genetic linkage map is a RFLP cDNA-based map, these data also provide a minimal estimate for the size of the euchromatic regions. The implications of these findings on positional cloning in *A. aegypti* are discussed.

DISEASE causing, arboviral, filarial and malarial parasites are transmitted to humans by mosquitoes from the subfamilies Culicinae and Anophelinae. Malaria, filariasis, and dengue fever are the three major causes of morbidity and mortality in developing countries. In the past the most successful control of these diseases has been through mosquito control programs. Efforts to control these diseases have become more difficult because malarial parasites have become drug resistant, mosquitoes have become insecticide resistant, and mosquito control programs have been discontinued or poorly supported.

Since the inheritance of filarial vector competence as a sex-linked recessive trait was demonstrated (MacDonald 1962a,b), vector competence has become the priority target for genetic and molecular studies. Research efforts have focused on map-based positional cloning of genes responsible for parasite vector competence in *Anopheles gambiae* and *Aedes aegypti*. In map-based cloning, the phenotype of interest is linked to a genetic map that is anchored to a physical map. Genomic libraries are screened for clones from the defined region, a contig map is constructed, and a transcript map is produced. Eventually a gene in the area is correlated with phenotype.

Corresponding author: D. L. Knudson, Department of Bioagricultural Sciences and Pest Management, College of Agricultural Sciences, Colorado State University, Fort Collins, CO 80523.
E-mail: dennis.knudson@colostate.edu

[1] *Present address:* Department of Biological Sciences, University of Notre Dame, Notre Dame, IN 46556.

A. aegypti and *An. gambiae* are the two most studied mosquito species. Aedes belongs to the subfamily Culicinae and has a genomic organization more similar to humans, whereas Anopheles belongs to the subfamily Anophelinae and has a genomic organization similar to Drosophila (Knudson *et al.* 1996). Although these mosquitoes both vector disease, that is where their similarity ends. Differences between these species have required very different strategies to initiate map-based cloning of the genes for vector competence.

Progress has been reported in the map-based cloning of the three genes in *An. gambiae* that control the encapsulation of malaria parasites. The construction of a low-resolution map was completed in 1991, using microdissection techniques pioneered in Drosophila (Zheng *et al.* 1991). The construction of a genetic map for *An. gambiae* moved slowly until microsatellite markers were used in the construction of genetic linkage maps. Recently the two maps were integrated either by the *in situ* hybridization of genetic markers to polytene chromosomes or the hybridization of genetic markers to polytene divisional pools (Dimopoulos *et al.* 1996; Zheng *et al.* 1993, 1996).

A. aegypti was the first mosquito species for which a detailed genetic linkage map was constructed. The initial genetic linkage map for *A. aegypti* (Craig and Hickey 1967; Munstermann and Craig 1979) has been expanded using restriction fragment length polymorphism (RFLP) cDNA-based markers (Severson *et al.* 1993, 1995a). The filarial vector competence phenotype has been demonstrated to be a quantitative trait, with the original f^m locus on chromosome 1 making the

largest contribution to the trait (Beerntsen *et al.* 1994; Severson 1994; Severson *et al.* 1994, 1995b; Thathy *et al.* 1994).

The physical map for *A. aegypti* has been difficult to generate because *A. aegypti* does not yield usable polytene chromosomes. Fluorescence *in situ* hybridization (FISH) techniques that were pioneered in the human genome project provided a strategy to overcome the lack of mappable polytenes in *A. aegypti*. We initially placed 37 random probes to the chromosomes of *A. aegypti* and found that landmarks were needed to identify the chromosomes and orient the chromosome arms (Brown *et al.* 1995). We constructed a single landmark probe from repetitive DNA that uniquely marked each of the three chromosomes with paired signals and with a distinct signal intensity (Brown and Knudson 1997). With these tools, we were ready to meet the challenge of integrating the maps. We report herein the first integrated genetic map for a Culicine mosquito, *A. aegypti*, using two FISH mapping approaches.

MATERIALS AND METHODS

Metaphase chromosome preparations: The cell line used as a source of genomic DNA and metaphase chromosome preparations was the *A. aegypti* continuous cell line, ATC-10, which is available from the American Type Culture Collection, designated as ATCC CCL-125. The cell line was maintained in 150-cm^2 flasks and grown in Leibovitz's L-15 media (GIBCO-BRL Life Technologies, Gaithersburg, MD) with 100 units/ml of penicillin and 100 μg/ml streptomycin (GIBCO-BRL Life Technologies), and 20% fetal bovine serum. The cell cultures were split 1:2 once a week. Metaphase chromosomes were prepared from *A. aegypti* ATC-10 cell cultures using standard cytogenetic procedures as described previously (Brown *et al.* 1995).

DNA and cosmid libraries: *A. aegypti* genomic DNA was isolated from the ATC-10 cell line following procedures described elsewhere (Ausubel *et al.* 1987) and plasmid DNA was purified using a rapid alkaline extraction (Birnboim and Doly 1979). Cosmid DNA purification, restriction endonuclease analysis with *Not*I, and contour-clamped homogeneous electric field (CHEF)-DR II gel electrophoresis (Bio-Rad Laboratories) followed standard protocols either described previously (Brown *et al.* 1995; Brown and Knudson 1997) or elsewhere (Ausubel *et al.* 1987). The cosmid library K6 was constructed from ATC-10 DNA using the SuperCos1 vector and host cell strain NM555 following previously described procedures, except that the library was not amplified (Brown *et al.* 1995). The cosmid library LSBC was constructed using *A. aegypti* Liverpool strain genomic DNA and the SuperCos1 vector in the host strain XL4-MK (D. W. Severson, unpublished data).

***In situ* hybridization, microscopy, and digital imaging:** Laboratory protocols for *in situ* hybridization reactions have been described in detail elsewhere (Ausubel *et al.* 1987; Brown *et al.* 1995). Briefly, probes were labeled with biotin-14-dATP using standard nick translation procedures. The labeled probe, C_ot-1 fraction, and salmon sperm DNA were sized to 100–500 bp (10 μg), precipitated, denatured at 80° for 10 min, and allowed to reanneal at 37° for 30 min. Slides containing metaphase chromosomes were treated separately to denature the chromosomal DNA, the preannealed probe was added to the slide, and hybridization occurred overnight. The excess probe was removed from the slides by several washes. The slides were blocked with 3% bovine serum albumin in 4× SSC and the biotinylated probe was detected with FITC-conjugated avidin; any excess was removed by a brief wash. The slides were counterstained with 4′,6-diamidino-2-phenylindole (DAPI; 0.2 μg/ml) and stored at 4° until examined optically. To simplify orientation of the chromosomes and signal measurements, a single plasmid, p2392, containing the chromosomal landmarks (Brown and Knudson 1997), was also nick-translated with digoxigenin-11-dUTP, added to the preannealed probe mix, and detected using rhodamine-conjugated anti-digoxigenin. Digital images were captured of the DAPI, FITC, and rhodamine-stained images using a cooled-array charged coupled device (CCD) and they were processed as described previously (Brown *et al.* 1995; Brown and Knudson 1997). Nonoverlapping chromosome spreads were examined for the position and intensity of the landmark probe and test FISH signals. Measurements were made of the short arm (*p*-arm), long arm (*q*-arm), and the total chromosome length; the FISH signal position was expressed as a percentage of fractional length (% FL) from the smaller arm or *p*-arm terminus (pter) relative to the total length of the chromosome (% FLpter).

Ultrasensitive FISH techniques: Prior to the denaturation step, slides were pretreated with RNAse (170 ng RNAse/1 μl 1× SSC) for 45 min at 37°. Denaturation and hybridization conditions were the same through the posthybridization washes. Amplification and detection procedures were as described in the tyramide signal amplification-indirect (ISH) manual [TSA-indirect (ISH), NEL730; New England Nuclear Life Science Products, Boston]. Slides were then blocked and detected with rhodamine, counterstained with DAPI, and mounted.

Sequencing, primer design, and sequence-tagged sites content mapping: cDNA RFLP marker sequences were reported elsewhere (Severson and Zhang 1996) and sequence information from the literature for some clones representing known genes in *A. aegypti* was also used. Optimal primers for sequence-tagged sites (STS) PCR screens were identified using the PRIMER computer program (Primer, v0.5; Whitehead Institute for Biomedical Research). The recombinant cosmid libraries were screened using a PCR-based STS screen. Synthetic oligonucleotide primers were tested by PCR with genomic DNA (10 ng/reaction), the RFLP clone (our positive control), and a negative control (no DNA template). Primers were designed to amplify sequences between 100 and 500 bp in total length and were easily visualized by electrophoresis in 1% agarose gels. Primer pairs that are distributed throughout the *A. aegypti* genome were identified and were representative of the ends of the genetic linkage map (Severson and Zhang 1996).

STS content mapping was accomplished through the PCR screens of pooled recombinant cosmids. Briefly, cosmid clones representing primary transfectants were grown in selective media and aliquots representing the individual clones were transferred to 96-well microtiter plates and stored at −80°. Additionally, equal aliquots of each clone in each plate were combined and subjected to standard cosmid DNA purification procedures. This provided us with individual DNA samples that contained all 96 clones (a plate pool) for each 96-well plate. Aliquots of DNA from the plate pool were then combined in a hierarchical manner that allowed us to conduct a primary screen of all cosmid clones for an RFLP marker sequence with only 5–10 PCR reactions. When one of these PCR reactions was positive for an STS marker, the 96-well plate containing the cosmid of interest was identified by PCR of the next hierarchical level of multiple plate pools. The specific cosmid was identified using two different approaches. In one approach, a 96-pin plate replicator was used to transfer and grow cosmids from the positive plate on a nylon membrane,

TABLE 1

Correlation of RFLP genetic linkage map with the FISH physical map of *Aedes aegypti*

Chromosome	Locus cDNA probe	Cosmid probe	Cosmid contains locus	cM	% cM	% FLpter	±SD	*n*
1		LSBC3.5	LF90	0.2	0.3	5.2	3.1	24
1		LSBC125.4O7	LF198	19.8	28.2	11.5	3.5	19
1	LF198			19.8	28.2	13.8	4.7	13
1	LF150			40.3	57.4	19.9	8.4	7
1		LSBC29.1	LF178	32.4	46.2	25.6	6.3	28
1	LF178[a]			32.4	46.2	26.9	4.6	8
1	LF179			45.9	65.4	27.6	5.0	6
1		LSBC101.1C9	*AeW*	29.2	41.6	29.7	5.0	13
1	LF99b			38.7	55.1	34.9	11.9	10
1		LSBC112.3E12	*Ace*	37.1	52.8	40.9	2.6	13
			Chromosome 1 total cM: 70.2					
2	LF115			0	0	0.3	—	2
2	*Rdl*			12.3	20.4	5.6	—	2
2		LSBC107.10G7	LF115	0	0	7.0	2.6	12
2	LF98[a,c]			20.0	33.1	12.6	4.9	20
2	LF181[b]			18.3	30.3	13.1	5.4	29
2	*AmyI*			23.0	38.1	15.3	2.9	7
2		LSBC119.9E2	LF124	32.1	53.1	28.9	6.9	9
2	LF180			28.6	47.4	33.7	4.9	8
2	LF355			36.0	59.6	77.9	5.7	7
2	LF223			60.4	100.0	89.5	6.8	9
2	*DDC*			43.6	72.2	93.4	5.7	10
2	*D7*			46.6	77.2	96.6	3.9	6
2	LF211			60.4	100.0	96.7	2.1	7
			Chromosome 2 total cM: 60.4					
3	LF347			0	0	4.2	2.0	5
3	LF227			17.1	30.0	13.0	5.7	6
3	LF99a			20.6	36.1	20.7	5.7	7
3	*MalF*			21.1	37.0	25.1	4.3	8
3		K6.2B3	LF108	37.9	66.5	73.7	1.9	4
3	*Apy*			57.0	100.0	80.6	7.4	8
3	LF323			43.5	76.3	83.1	4.5	6
			Chromosome 3 total cM: 57.0					
			RFLP linkage map total cM: 87.6					

cM, Kosambi centimorgan units of the locus position in the genetic linkage map (Severson *et al.* 1993; D. W. Severson, unpublished data); % cM, the locus position in the genetic linkage map as a percentage; % FLpter, percentage fractional length from the smaller *p*-arm terminus relative to the total length of the chromosome; SD, standard deviation of the % FLpter measurement; and *n*, the number of % FLpter measurements made; these measurements may have come from one or more hybridization reactions.

[a] QTL anchor marker for two QTL that affect susceptibility to the filarial worm *Brugia malayi* (Severson *et al.* 1994).

[b] QTL anchor marker for a QTL that has been associated with midgut penetration by *B. malayi* microfilarie (Beerntsen *et al.* 1995).

[c] QTL anchor marker for two QTL that affect susceptibility to the malarial parasite, *Plasmodium gallinaceum* (Severson *et al.* 1995b).

which was then probed with the radiolabeled STS fragment. In the second approach, row and column pools were made from the plate of interest and these 20 pools were screened by PCR with the primers to identify the intersection of the row and column pools.

RESULTS AND DISCUSSION

We have taken two FISH approaches toward reconciling the *A. aegypti* genetic and physical maps and both approaches involved hybridization of genetic marker sequences to the chromosomes in the presence of a landmark probe. The landmark probe allowed the chromosomes and the chromosome arms to be identified so that the location of the genetic marker sequences could be determined accurately and quickly. The landmark probe produces the strongest signal on chromosome 1 at 71% FLpter, the next most intense signal on chromosome 2 at 96% FLpter, and the lightest signal

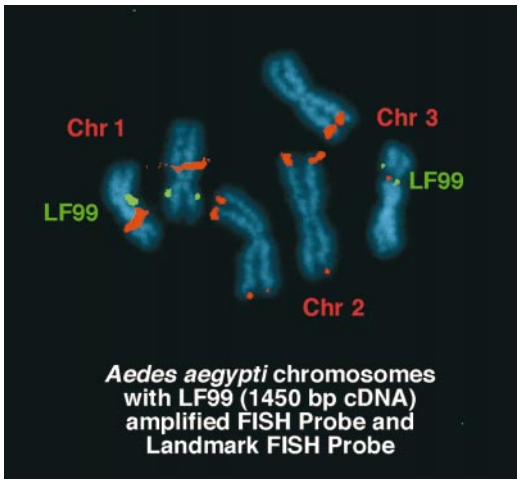

Figure 1.—Mapping of a cDNA clone using ultrasensitive FISH techniques. A photomicrograph of FISH with a labeled cDNA clone to *Aedes aegypti* metaphase chromosomes is depicted. The biotin-labeled cDNA LF99 was detected using the TSA-indirect amplification technique with streptavidin fluorescein conjugate. The landmark probe p2392 was labeled with digoxigenin-11-dUTP and detected using rhodamine-conjugated anti-digoxigenin. The landmark probe allowed the chromosomes to be identified as indicated in red and oriented relative to the *p*-arm, the starting point of all % FLpter measurements. Digital images were captured and processed as described (Brown *et al.* 1995; Brown and Knudson 1997). LF99 has two loci (see Table 1 and Severson *et al.* 1993), LF99a on linkage group 3 and LF99b on the linkage group 1; FISH using LF99 results in signals at 35% FLpter on the *p*-arm of chromosome 1 and at 21% FLpter on the *q*-arm of chromosome 3. The cDNA signal is colored green and the landmark probe is colored red. Note that LF99a maps at the previously described break-point on chromosome 3 (Brown *et al.* 1995; Brown and Knudson 1997) with the LF99a signal seen on either side. The LF99a signal on the other homologue is obscured by the landmark signal. The position of LF99b on chromosome 1 is readily discernible on one homologue and less well defined on the other.

on chromosome 3 at 86% FLpter (Brown and Knudson 1997). The sequence of the landmark probe has been reported (Brown and Knudson 1997).

The first approach follows the well-accepted strategy of using an STS procedure to screen our cosmid libraries (Green and Green 1991). Once a cosmid containing a specific STS was identified, it was physically mapped using standard FISH procedures, thereby anchoring it to a specific chromosomal location. Initially, we tried to choose STS markers that provided the most complete coverage of the current genetic linkage map (Severson *et al.* 1993; D. W. Severson, unpublished data), thereby spanning the entire genetic map. We isolated cosmids that contained eight RFLP marker sequences that had been located on the genetic linkage map (Table 1). The markers contained in cosmids were LF90, LF198, LF178, *AeW*, *Ace*, LF115, LF124, and LF108. This approach is quite effective in placing markers on the map, but there are some disadvantages. For example, the library must cover the genome multiple times to have a high enough probability of finding one's marker, the PCR-based screening is expensive, and the labor and time involved in PCR-based screening are high.

In a second more direct approach, we attempted to FISH map cDNA clones representing RFLP markers directly to metaphase chromosomes. Generally, FISH using smaller probes such as cDNAs does not reliably produce signals. That is, cDNA-sized probes have not been useful as FISH probes unless there are multiple local copies of the gene or polytene chromosomes available. The problem is that, using standard FISH procedures, small probes (<5 kb) do not incorporate sufficient signal for detection even with the use of exquisitely sensitive CCD image capture systems. We were, however, able to successfully adapt a FISH amplification procedure (Raap *et al.* 1995) for mapping cDNA-sized probes to metaphase chromosomes of *A. aegypti*. The TSA-indirect procedure amplifies the fluorescent signals as much as a 1000-fold. In this indirect procedure streptavidin horseradish peroxidase (SA-HRP) attaches to biotin and catalyzes the deposition of numerous molecules of biotinyl tyramide onto the chromosomes, which are then detected with a conjugated streptavidin fluorescein. This development opened the way for mapping of cDNAs directly. We have successfully mapped 21 cDNAs, representing RFLP markers, directly to metaphase chromosomes using the amplified FISH procedure with 5 cDNAs on chromosome 1, 11 on chromosome 2, and 6 on chromosome 3 (Table 1). The smallest cDNA we have mapped using TSA-indirect was LF347, a 400-bp probe. Specific FISH signals for the LF99 cDNA probe (Table 1) may be seen on chromosomes 1 and 3 (Figure 1). This result is not surprising because LF99 has two loci (see Table 1 and Severson *et al.* 1993), LF99a and LF99b, which are located on the linkage groups 3 and 1, respectively.

Three of the genetic markers were physically mapped by both approaches. LF198, LF178, and LF115 were mapped directly and by using cosmids that contained them. LF198 and LF178 were mapped to the same location using both techniques. The number of observations for each technique with these markers was in excess of five. LF115 hybridized to chromosome 2 with both approaches. However, standard deviations of their positions by the two techniques did not overlap. This discrepancy is probably due to the small sample size (two) using the TSA-indirect technique for LF115.

Of the 22 cDNA markers that were put to the physical map, 6 were known genes. The known genes that mapped to chromosome 2 were *Rdl*, cyclodiene resistance (Thompson *et al.* 1993); *AmyI*, salivary gland amylase (Grossman and James 1993); *DDC*, dopa decarboxylase (Ferdig *et al.* 1996); and *D7*, salivary gland protein (James *et al.* 1991). Known genes that were physically mapped to chromosome 3 were *MalI*, maltase-like enzyme (James *et al.* 1989); and *Apy*, apyrase (Champagne

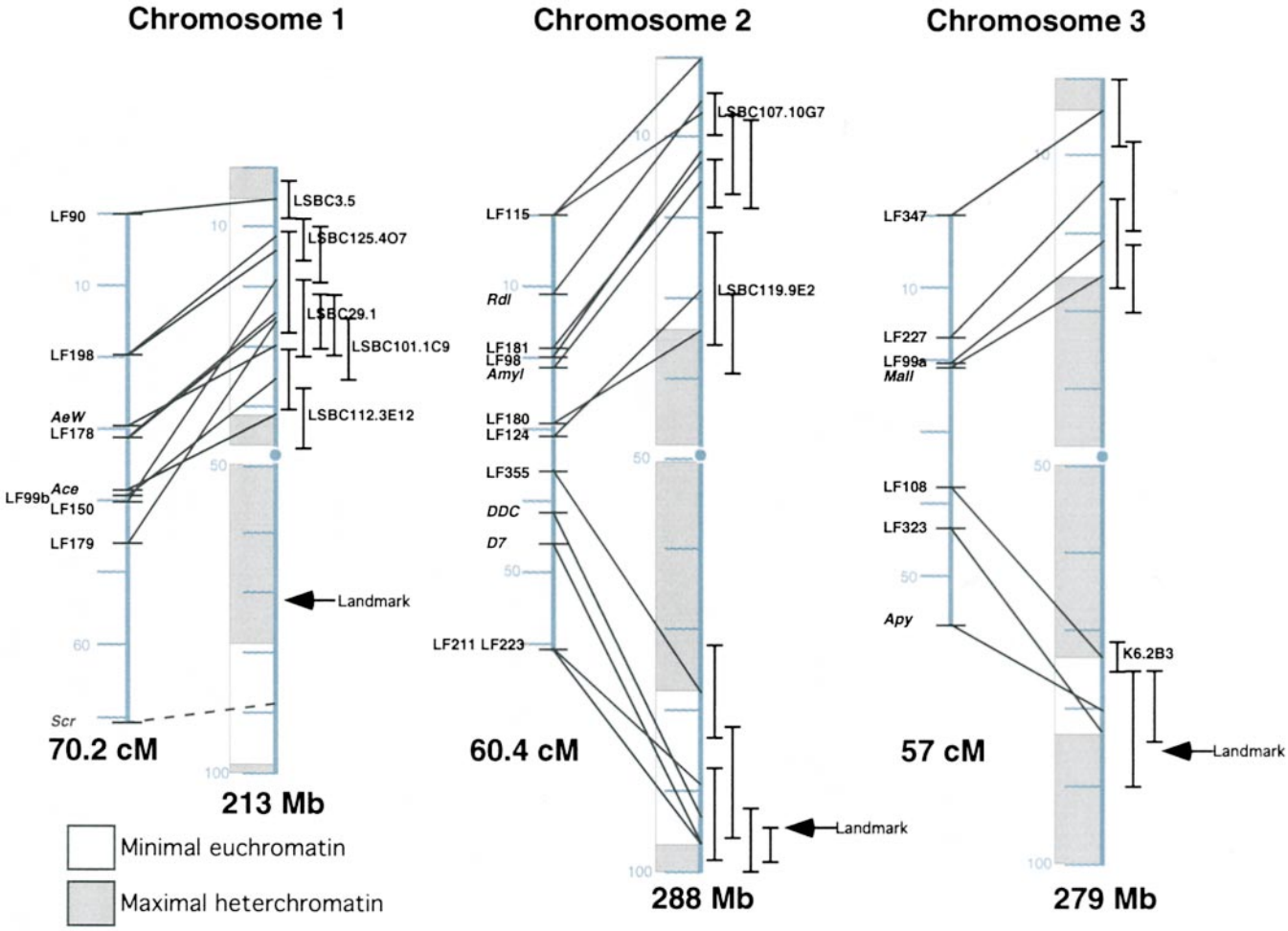

FIGURE 2.—Integration of the genetic linkage maps and the physical map of *Aedes aegypti*. A graphical representation of the integrated genetic and physical map is presented (see Table 1). The genetic linkage map is in centimorgans (cM) whereas the physical map is in megabases (Mb). Heavy lines link the genetic loci to their appropriate locations on the physical map. When a cosmid clone was found using STS primers for a specific cDNA locus, its position is indicated at the center point of the FISH % FLpter standard deviation error bars on the physical map. When only the cDNA locus was used as the probe, its position is noted on the genetic linkage map (SEVERSON *et al.* 1993; D. W. SEVERSON, unpublished data). Multiple measurements were made for each probe that was put to the physical map (see Table 1); therefore the clone was placed at the middle of its standard deviation error bars. The linear order for loci between the two maps is consistent with minor loci inversions. The chromosome numberings for the two maps correspond; however, the genetic linkage map does not entirely cover chromosomes 1 and 3. The genetic linkage map is a RFLP cDNA-based map, and, thus, these data also provide a minimal estimate for the size of the euchromatic and heterochromatic regions as indicated by open and shaded blocks. Since the distal end of linkage group 1 was not represented in this study, our estimated position is indicated by the dotted line linking the linkage map with the physical map (see text for discussion).

et al. 1995). Putative identification of additional cDNA markers used in this study was made by database comparisons. High amino acid homologies were made for LF198, NADH-ubiquinone reductase, LF178, human QM protein (a putative tumor repressor protein), and LF115, ribosomal protein L18 (SEVERSON and ZHANG 1996).

The integration of the genetic linkage map and the FISH physical map of metaphase chromosomes is depicted in Figure 2. Linear orders for loci on each chromosome are consistent between the two maps, with only some apparent local inversions in order. Such slight inconsistencies have commonly been observed with other organisms, with the correct order usually being reflected by the physical map data. That is, genetic linkage associations are based on statistical estimates of recombination and not all our RFLP markers have been tested directly in the same mapping population. In those instances where probe % FLpter standard deviations overlap, fine-scale FISH mapping may be used later to unequivocally confirm their order. This approach is best accomplished by using multiple probes, each tagged with a unique fluor that may be discriminated simultaneously in a single hybridization reaction (SPEICHER *et al.* 1996). We have successfully used three fluors, fluorescein, Cy3, and Cy5, in a single hybridization reaction

TABLE 2

Relationship of Mb/cM

	Chromosome		
	1	2	3
Relative genome size[a] (%)	27.3	36.9	35.8
Mb[b]	213	288	279
cM	70.2	60.4	57
cM on physical map (%)	65	100	100
Physical map representing cM (%)	36	97	83
Small arm (*p*-arm) interval Mb/cM	1.7	3.0	2.8
Large arm (*q*-arm) interval Mb/cM	—	2.2	1.4
Minimal euchromatic region	117 Mb[c]	150 Mb	85 Mb
Maximal heterochromatic region	96 Mb[c]	138 Mb	194 Mb

[a] Based on length measurements.

[b] Haploid genome (780 Mb), calculated from the 0.8 pg/haploid genome (Warren and Crampton 1991; Knudson *et al.* 1996) and 980 Mb/pg.

[c] See text for discussion of the additional 41-Mb euchromatic region on the *q*-arm of chromosome 1 that has been added to the euchromatic region and subtracted from heterochromatin.

to confirm the order of three probes (S. E. Brown and D. L. Knudson, unpublished data).

The chromosome numbering schemes of the genetic and physical maps correspond; that is, chromosome 1 is the same in both maps. The published graphical orientations of the linkage maps for chromosomes 2 and 3 were inverted when compared to the physical map. The linkage maps for these two chromosomes now follow the physical map orientation (Table 1 and Figure 2; see also AaeDB at Mosquito Genomics WWW Server, at http://klab.agsci.colostate.edu). Sixty-five percent of the chromosome 1 genetic linkage map is located physically within 36% on the short *p*-arm (Table 2). For chromosome 2, 100% of the genetic linkage map is found across both arms or within 97% of the physical length. For chromosome 3, 100% of the genetic linkage map is found across both arms as well, but 83% of the physical map contains the complete chromosome 3 genetic linkage map. Since the genetic linkage map is a RFLP cDNA-based map, these data also provide a minimal estimate for the size of the euchromatic regions (Table 2 and Figure 2). Since 35% of linkage group 1, or 24.3 cM from the distal end, was not represented in this study, it is unlikely that the *q*-arm of chromosome 1 is entirely heterochromatic (Figure 2) and there are observations in support of this perspective. For example, the ferritin gene was placed recently to chromosome 1 at 88% FLpter (Pham *et al.* 2000). Further, the *Scr* marker at the distal end of the linkage group 1 is a homeobox-related gene. We have FISH mapped a number of other homeobox-related cDNAs with variable results, but several seemed to be located on the *q*-arm of chromosome 1 (S. E. Brown and D. L. Knudson, unpublished data). In addition, the repetitive ribosomal cistron (rDNA locus) maps to 71% FLpter and is the chromosome 1 landmark (see Figures 1 and 2; Brown and Knudson 1997). In Figure 2, we have represented an interpreted euchromatic region on the *q*-arm of chromosome 1 (dotted line on chromosome 1 in Figure 2). Hence, these integration studies provide strong evidence that the genetic linkage map is highly representative of the euchromatic regions found in the *A. aegypti* genome.

Given the genome size estimate of 780 Mb (see Table 2) and these integration data, then the minimal euchromatic portion of the genome is at least 311 Mb in size and the maximal size for the heterochromatin would be 469 Mb. In addition, we would increase our estimate to include ~41 Mb of euchromatin at the distal end of the *q*-arm of chromosome 1 (dotted line on chromosome 1 in Figure 2). Hence, the total minimal euchromatic region estimate would be 352 Mb and the maximal heterochromatin would be 428 Mb or 45 and 55%, respectively (Figure 2). Our overall estimate of megabases per centimorgan is 2.1 across the euchromatic regions identified in all three chromosomes (Table 2) and this number is within the range of those reported for other organisms.

The integrated genetic and physical maps for *A. aegypti* provide a sound platform for our efforts to use positional cloning to isolate genes determining vector competence for two parasite species. This study physically placed several anchor markers for each of these quantitative trait loci (QTL; Table 1). This includes marker loci for two QTL that affect susceptibility to the malarial parasite *Plasmodium gallinaceum* (Severson *et al.* 1995b), two QTL that affect susceptibility to the filarial worm *Brugia malayi* (Severson *et al.* 1994), and a QTL that has been associated with midgut penetration by *B. malayi* microfilariae (Beerntsen *et al.* 1995).

We have presented the first integrated genetic linkage and physical map for *A. aegypti*. We have also provided

evidence that the genetic linkage map is representative of the euchromatic region of the genome, demonstrated that large regions of the physical map likely represent heterochromatin, and located the euchromatin and heterochromatin on the physical map. This finding has implications for positional cloning as only 45% of the genome seems to be transcriptionally active. The integrated map will be the foundation for our ongoing map-based cloning studies of the QTL that affect vector competence of filarial and malarial parasites in *A. aegypti*.

The expert technical assistance of Susan H. Harris is acknowledged. John Harris is acknowledged for his assistance with digital imaging. The laboratory support services of P. Carlson, S. C. Deeney, L. A. Kempton, M. Kempton, and M. A. Lawrenz are also acknowledged. This work was supported by the National Institutes of Health, National Institute of Allergy and Infectious Disease grant AI34337, in part by the MacArthur Foundation through their Research Network on the Biology of Parasite Vectors program, and in part by the Colorado Agricultural Experiment Station.

LITERATURE CITED

Ausubel, F. M., R. Brent, R. E. Kingston, D. D. Moore, J. G. Seidman *et al.*, (Editors), 1987 *Current Protocols in Molecular Biology*. Greene Publishing Associates and Wiley-Interscience, New York.

Beerntsen, B. T., D. W. Severson and B. M. Christensen, 1994 *Aedes aegypti*: characterization of a hemolymph polypeptide expressed during melanotic encapsulation of filarial worms. Exp. Parasitol. **79:** 312–321.

Beerntsen, B. T., D. W. Severson, J. A. Klinkhammer, V. A. Kassner and B. M. Christensen, 1995 *Aedes aegypti*: a quantitative trait locus (QTL) influencing filarial worm intensity is linked to QTL for susceptibility to other mosquito-borne pathogens. Exp. Parasitol. **81:** 355–362.

Birnboim, H. C., and J. Doly, 1979 A rapid alkaline extraction procedure for screening recombinant plasmid DNA. Nucleic Acids Res. **7:** 1513–1523.

Brown, S. E., and D. L. Knudson, 1997 FISH landmarks for *Aedes aegypti* chromosomes. Insect Mol. Biol. **6:** 197–202.

Brown, S. E., J. Menninger, M. Difillipantonio, B. J. Beaty, D. C. Ward *et al.*, 1995 Toward a physical map of *Aedes aegypti*. Insect Mol. Biol. **4:** 161–167.

Champagne, D. E., C. T. Smartt, J. M. Ribeiro and A. A. James, 1995 The salivary gland-specific apyrase of the mosquito *Aedes aegypti* is a member of the 5′-nucleotidase family. Proc. Natl. Acad. Sci. USA **92:** 694–698.

Craig, G. B., Jr., and W. A. Hickey, 1967 Genetics of *Aedes aegypti*, pp. 67–131 in *Genetics of Insect Vectors of Disease*, edited by J. W. Wright and R. Pal. Elsevier Publishing Company, Amsterdam.

Dimopoulos, G., L. Zheng, V. Kumar, A. della Torre, F. C. Kafatos *et al.*, 1996 Integrated genetic map of *Anopheles gambiae*: use of RAPD polymorphisms for genetic, cytogenetic and STS landmarks. Genetics **143:** 953–960.

Ferdig, M. T., J. Li, D. W. Severson and B. M. Christensen, 1996 Mosquito dopa decarboxylase cDNA characterization and blood-meal-induced ovarian expression. Insect Mol. Biol. **5:** 119–126.

Green, E. D., and P. Green, 1991 Sequence-tagged site (STS) content mapping of human chromosomes: theoretical considerations and early experiences. PCR Methods Appl. **1:** 77–90.

Grossman, G. L., and A. A. James, 1993 The salivary glands of the vector mosquito, *Aedes aegypti*, express a novel member of the amylase gene family. Insect Mol. Biol. **1:** 223–232.

James, A. A., K. Blackmer and J. V. Racioppi, 1989 A salivary gland-specific, maltase-like gene of the vector mosquito, *Aedes aegypti*. Gene **75:** 73–83.

James, A. A., K. Blackmer, O. Marinotti, C. R. Ghosn and J. V. Racioppi, 1991 Isolation and characterization of the gene expressing the major salivary gland protein of the female mosquito, *Aedes aegypti*. Mol. Biochem. Parasitol. **44:** 245–254.

Knudson, D. L., L. Zheng, S. W. Gordon, S. E. Brown and F. C. Kafatos, 1996 Genome organization of vectors, pp. 175–214 in *The Biology of Disease Vectors*, edited by B. J. Beaty and W. C. Marquardt. University Press of Colorado, Niwot, CO.

MacDonald, W. W., 1962a The genetic basis of susceptibility to infection with semi-periodic *Brugia malayi* in *Aedes aegypti*. Ann. Trop. Med. Parasitol. **56:** 373–382.

MacDonald, W. W., 1962b The selection of a strain of *Aëdes aegypti* susceptible to infection with semi-periodic *Brugia malayi*. Ann. Trop. Med. Parasitol. **56:** 368–372.

Munstermann, L. E., and G. B. Craig, Jr., 1979 Genetics of *Aedes aegypti*: updating the linkage map. J. Hered. **70:** 291–296.

Pham, D. Q.-D., S. E. Brown, D. L. Knudson, J. J. Winzerling, M. S. Dodson *et al.*, 2000 Structure and location of the ferritin gene of the yellow fever mosquito *Aedes aegypti*. Eur. J. Biochem. **267:** 1–7.

Raap, A. K., M. P. C. van de Corput, R. A. W. Vervenne, R. P. M. van Gijlswijk, H. J. Tanke *et al.*, 1995 Ultra-sensitive FISH using peroxidase-mediated deposition of biotin- or fluorochrome tyramides. Hum. Mol. Genet. **4:** 529–534.

Severson, D. W., 1994 Applications of molecular marker analysis to mosquito vector competence. Parasitol. Today **10:** 336–340.

Severson, D. W., and Y. Zhang, 1996 Generation of expressed sequence tags and sequence-tagged sites as physical landmarks in the mosquito, *Aedes aegypti*, genome. Genome **39:** 224–229.

Severson, D. W., A. Mori, Y. Zhang and B. M. Christensen, 1993 Linkage map for *Aedes aegypti* using restriction fragment length polymorphisms. J. Hered. **84:** 241–247.

Severson, D. W., A. Mori, Y. Zhang and B. M. Christensen, 1994 Chromosomal mapping of two loci affecting filarial worm susceptibility in *Aedes aegypti*. Insect Mol. Biol. **3:** 67–72.

Severson, D. W., A. Mori, V. A. Kassner and B. M. Christensen, 1995a Comparative linkage maps for the mosquitoes, *Aedes albopictus* and *Ae. aegypti* based upon common RFLP loci. Insect Mol. Biol. **4:** 41–45.

Severson, D. W., V. Thathy, A. Mori, Y. Zhang and B. M. Christensen, 1995b Restriction fragment length polymorphism mapping of quantitative trait loci for malaria parasite susceptibility in the mosquito *Aedes aegypti*. Genetics **139:** 1711–1717.

Speicher, M. R., S. Gwyn Ballard and D. C. Ward, 1996 Karyotyping human chromosomes by combinatorial multi-fluor FISH. Nat. Genet. **12:** 368–375.

Thathy, V., D. W. Severson and B. M. Christensen, 1994 Reinterpretation of the genetics of susceptibility of *Aedes aegypti* to *Plasmodium gallinaceum*. J. Parasitol. **80:** 705–712.

Thompson, M., J. C. Steichen and R. H. ffrench-Constant, 1993 Conservation of cyclodiene insecticide resistance-associated mutations in insects. Insect Mol. Biol. **2:** 149–154.

Warren, A. M., and J. M. Crampton, 1991 The *Aedes aegypti* genome: complexity and organization. Genet. Res. **58:** 225–232.

Zheng, L., R. D. C. Saunders, D. Fortini, A. della Torre, M. Coluzzi *et al.*, 1991 Low-resolution genome map of the malaria mosquito *Anopheles gambiae*. Proc. Natl. Acad. Sci. USA **88:** 11187–11191.

Zheng, L., F. H. Collins, V. Kumar and F. C. Kafatos, 1993 A detailed genetic map for the X chromosome of the malaria vector, *Anopheles gambiae*. Science **261:** 605–608.

Zheng, L., M. Q. Benedict, A. J. Cornel, F. H. Collins and F. C. Kafatos, 1996 An integrated genetic map of the African human malaria vector mosquito, *Anopheles gambiae*. Genetics **143:** 941–952.

Communicating editor: G. B. Golding